Journal of Integrative Agriculture 2023, 22(6): 1618–1630

Available online at www.sciencedirect.com

ScienceDirect

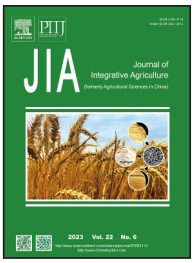

RESEARCH ARTICLE

Variations in chlorophyll content, stomatal conductance, and photosynthesis in *Setaria* EMS mutants

TANG Chan-juan*, LUO Ming-zhao*, ZHANG Shuo, JIA Guan-qing, TANG Sha, JIA Yan-chao, ZHI Hui, DIAO Xian-min#

Institute of Crop Sciences, Chinese Academy of Agricultural Sciences, Beijing 100081, P.R.China

Abstract

Chlorophyll (Chl) content, especially Chl *b* content, and stomatal conductance (G_s) are the key factors affecting the net photosynthetic rate (P_n). *Setaria italica*, a diploid C_4 panicoid species with a simple genome and high transformation efficiency, has been widely accepted as a model in photosynthesis and drought-tolerance research. The current study characterized Chl content, G_s, and P_n of 48 *Setaria* mutants induced by ethyl methanesulfonate. A total of 24, 34, and 35 mutants had significant variations in Chl content, G_s, and P_n, respectively. Correlation analysis showed a positive correlation between increased G_s and increased P_n, and a weak correlation between decreased Chl *b* content and decreased P_n was also found. Remarkably, two mutants behaved with significantly decreased Chl *b* content but increased P_n compared to Yugu 1. Seven mutants behaved with significantly decreased G_s but did not decrease P_n compared to Yugu 1. The current study thus identified various genetic lines, further exploration of which would be beneficial to elucidate the relationship between Chl content, G_s, and P_n and the mechanism underlying why C_4 species are efficient at photosynthesis and water saving.

Keywords: photosynthetic capacity, chlorophyll content, stomatal conductance, EMS mutant variation, *Setaria italica*

1. Introduction

Biomass synthesized *via* photosynthesis is the primary determinant of plant productivity. Improving photosynthetic performance, therefore, is of great importance to drive necessary gains in crop yield (Ort *et al.* 2015; Chabrand *et al.* 2016; Nowicka *et al.* 2018; Faralli and Lawson 2020). Chlorophyll (Chl) *a* and *b* are the most abundant pigments in the light-harvesting antenna system of higher plants; they play a central role in absorbing light and transmitting energy (Bjorn *et al.* 2009; Wang and Grimm 2015; Gitelson *et al.* 2016; Kume *et al.* 2018). In higher plants, the light-harvesting antenna system consists of a core antenna complex and several peripheral antenna complexes. Chl *a* occurs universally in all antenna complexes (including photosystem I (PSI) and PSII core complexes and peripheral antenna complexes), whereas Chl *b* is found nearly exclusively in the light-harvesting Chl *a*/*b*-protein complexes (LHCs) that form the peripheral antenna complexes (the PSI core

Received 3 June, 2022 Accepted 18 August, 2022
TANG Chan-juan, E-mail: 1406044224@qq.com; #Correspondence DIAO Xian-min, E-mail: diaoxianmin@caas.cn
* These authors contributed equally to this study.

doi: 10.1016/j.jia.2022.10.014

and PSII core almost completely lacks Chl *b*) (Kunugi *et al.* 2016; Kume *et al.* 2018). Changes in antenna size largely depend on LHCs abundance. For the amount of core complex per reaction center is fixed, whereas the organization of LHCs and peripheral antenna complexes is flexible among different photosynthetic organisms and under different solar conditions. According to Jia *et al.* (2016), levels of LHCII and antenna size were highly correlated with the accumulation of Chl *b*. Plants with increased Chl *b* accumulation assembled more LHCII complexes and had a larger antenna size (Tanaka and Tanaka 2011; Jia *et al.* 2016). Chl *b* content and the Chl *a*/*b* ratio, therefore, are useful as an index to indicate the LHCII abundance and antenna size of plants and are key parameters that determine light absorbing efficiencies (Bailey *et al.* 2001; Jia *et al.* 2016; Kume *et al.* 2018).

Tanaka *et al.* (2001) reported that overexpression of chlorophyllide a oxygenase (CAO) increased the synthesis of Chl *b* from Chl *a*, reducing the Chl *a*/*b* ratio from 2.85 to 2.65 and resulting in at least a 10–20% increase in the antenna size in *Arabidopsis thaliana* (Tanaka R *et al.* 2001). Genetic modification of the biosynthesis of Chl *b* in tobacco (*Nicotiana tabacum*) also revealed that increased Chl *b* synthesis in CAO-overexpressing plants increased antenna size, CO_2 assimilation, and dry matter accumulation, suggesting that engineering plants for larger antennae with higher Chl *b* content and lower Chl *a*/*b* ratio might have the potential for increasing photosynthesis, especially under low-light conditions (Biswal *et al.* 2012). However, higher plants, in which large arrays of LHCs are assembled as peripheral components of PSI and PSII, are highly efficient at absorbing and transferring photons, an arrangement that allows them to operate under dim light conditions but which can lead to excess energy accumulation in full sunlight (Rooijen *et al.* 2015; Chmeliov *et al.* 2016; Kromdijk *et al.* 2016). The excess energy should then be released as heat *via* nonchemical quenching mechanisms to protect the plant from photo-induced damage (Horton and Ruban 2005; Chmeliov *et al.* 2016; Kromdijk *et al.* 2016). Thus, a concept was proposed by Kirst *et al.* (2017) to develop a truncated light-harvesting chlorophyll antenna (TLA) to alleviate excess absorption of sunlight and the waste of excitation energy consumed by non-photochemical quenching in order to improve productivity. Prior research in *Chlamydomonas* has provided early evidence that a truncated light-harvesting antenna size could increase photosynthetic productivity in high-density cultures under bright sunlight conditions (Polle *et al.* 2003; Kirst *et al.* 2012; Mitra *et al.* 2012; Kirst and Melis 2014; Jeong *et al.* 2017). Subsequent research on tobacco reported a TLA material, in which Chl *a* and *b* contents were lowered to about 57 and 23% of wild type, respectively, and the Chl *a*/*b* ratio was elevated from about 3:1 to 8:1, which showed a 25% increase in stem and leaf biomass accumulation (Kirst *et al.* 2017). Slattery *et al.* (2017) reported that Chl deficiency in a soybean mutant line, *Y11y11*, led to greater rates of leaf-level photosynthesis per absorbed photon early in the growing season when mutant Chl content was ~35% of the wild type. Although research on reducing Chl content to increase light-use efficiency and yield improvements has not yet been seen in cereal crops, it becomes increasingly clear that optimizing light-harvesting management, such as modifying the antenna size and Chl biosynthesis, should be a focus of research for future improvement in photosynthesis and crop productivity (Ort *et al.* 2011; Song *et al.* 2017).

Increased stomatal conductance (G_s) has been a selective trait over decades in breeding for high-yielding varieties. As stomata govern the diffusion of CO_2 from the atmosphere to the leaf interior, it greatly influences CO_2 fixation in the mesophyll tissue (Lawson and Blatt 2014; Faralli *et al.* 2019). Over the long term and under steady conditions, increased G_s always strongly correlate with higher photosynthetic performance (Wong *et al.* 1979; Faralli *et al.* 2019). However, stomata also govern the diffusion of H_2O from the leaf interior to the atmosphere. Under low soil water conditions, crops tend to reduce G_s to reduce water consumption, thus leading to lower net photosynthetic rate (P_n) and depressed productivity (Gilbert *et al.* 2011). Therefore, it is important to balance gains in P_n with performance under drought stress (Chabrand *et al.* 2016; Golec *et al.* 2019). It is reported that both C_3 and C_4 plants are suffering from a decline in G_s and thus decreased intercellular CO_2 concentration (C_i) in the early phase of water stress (Israel *et al.* 2022). However, as C_4 plants are featured by an efficient CO_2-concentrating mechanism which enables them to saturate C_4 photosynthesis under relatively low C_i, C_4 plants thus may not decline CO_2 assimilation rates under the limited G_s as C_3 plants (Israel *et al.* 2022; Taylor *et al.* 2018). Pinto *et al.* (2014) reported that minor reductions of photosynthesis were produced in C_4 plants relative to C_3 and C_3–C_4 species under a lower CO_2 concentration. And according to Pinto *et al.* (2014), the initial decline of C_i to 50% to that of the control would not reduce CO_2 assimilation rates during the early phases of water stress in maize and amaranthus. A C_4 photosynthetic model described by Siebke (2002) also indicated that little influence would have on CO_2 assimilation rates even if C_i declined down to 50 Pa. It is therefore concluded that the efficient CO_2-concentrating mechanism is key for C_4 plants to maintain relatively higher photosynthesis

under water stress. Moreover, screening for mutants with few reductions in photosynthesis under restricted G_s in C_4 plants should be brought into focus for research on acclimating crops to drought conditions and improving crop yields.

Setaria italica, a diploid C_4 panicoid species with small stature, a simple genome of 430 Mb, and high transformation efficiency, has been a useful tool for functional gene mining and research, especially for genes involved in photosynthesis and drought resistance (Brutnell *et al.* 2010; Li and Brutnell 2011; Li *et al.* 2016; Diao *et al.* 2014; Huang *et al.* 2014; Tang *et al.* 2017; Luo *et al.* 2018; Doust *et al.* 2019; Nguyen *et al.* 2020; Pegler *et al.* 2020; Sood *et al.* 2020). In the current study, the Chl content of 28 leaf-color *Setaria* mutants and the photosynthetic performance of those mutants plus a further 20 mutants were characterized, aiming at providing a reference for modulating Chl content and G_s to improve drought tolerance and photosynthetic efficiency in major crops.

2. Materials and methods

2.1. Materials and growth conditions

Plant materials used for analyzing Chl and photosynthesis were derived from an ethyl methanesulfonate (EMS)-derived *Setaria italica* mutant library as previously described (Luo *et al.* 2018). Among the 2 709 M3/M4 lines, 28 were identified as leaf color mutants using a microscope, as described by Luo *et al.* (2018), and were compared with the wild-type Yugu 1. In addition to the 28 leaf color mutants, another 20 mutants (a total of 48 lines) were identified that might have variations in photosynthetic performance, as described by Luo *et al.* (2018), and therefore were subjected to photosynthesis analysis.

Experiments were conducted between July and September 2016 in the greenhouse of the Institute of Crop Sciences, Chinese Academy of Agricultural Science, Beijing, China (40°N, 116°E). The growth temperature of the greenhouse was in a range of 30 to 38°C. The artificial light was turned on at 8 a.m. and turned off at 6 p.m. Plants were grown in 3 m×0.9 m plots with a row space of 0.3 m and a space in the rows of 5 cm, using standard agronomic practices (e.g., irrigation, weeding, and pest control).

2.2. Chlorophyll analysis

Leaf tissues were taken from fully developed flag leaves about 5 d before flowering (50 d after seeding). A hole puncher was used to obtain 100 pieces of tissue of 3-mm diameter from the middle zone of the flag leaves. Foil-wrapped 10 mL centrifuge tube and carton were used to keep samples in the dark. For each material, six replicates were made. The leaf tissues were placed into 80% acetone and shaken for 24 h until the tissue color had completely faded. Finally, the solutions were placed in a UV-1800 ultraviolet/visible light spectrophotometer to measure their absorbance at 663 and 645 nm. The contents of Chl *a* and Chl *b* were then calculated using the formula described by Lichtenthaler (1987) :

$$\text{Chl } a = 12.25OD_{663} - 2.79OD_{645}$$

$$\text{Chl } b = 21.50OD_{645} - 5.10OD_{663}$$

$$\text{CV} = \text{Chl } a + \text{Chl } b$$

$$\text{CA (mg dm}^{-2}) = 0.1 \times \text{V (mL)} \times \text{CV/S (cm}^2)$$

where V is the volume of the 80% acetone for each replicate and S is the area of the leaf tissue for each replicate.

2.3. Photosynthesis analysis

The photosynthetic performance of the 48 mutants was measured using the LI-6400 photosynthesis system with a red-blue light source and 6-cm^2 cuvette (LI-6400XT, LI-COR, USA). For each line, we used at least 10 flag leaves of 50-day-old plants with the same height and orientation that allowed them to receive full light. Measurements were taken from 9:30 to 11:30 a.m. during 8–13 August. Cuvette conditions were: photosynthetic photon flux density, 1 500 μmol m^{-2} s^{-1}; sample CO_2 concentration, 400 μmol mol^{-1}; flow rate, 500 mL s^{-1}, and the cuvette fan was set to fast. The cuvette was placed in the middle leaf zone. Before logging the measurement, the criteria for stability are that parameters in line a are stable, parameters in line c are normal, fluctuation of ΔCO_2 in line b<0.2 μmol mol^{-1}, and one digit behind the decimal point of Photo is stable.

To minimize the effect of varied light, temperature, and vapor pressure deficit (Vpd) on the photosynthetic parameters obtained at different times, we carefully controlled the environmental conditions that might affect photosynthetic performance. Specifically, we chose sunny days with comparable solar radiation intensity, temperature, and humidity to do measurements and recorded photosynthetic parameters only when leaf temperature and Vpd reached 39 to 41°C and 4.5 to 5.5 kPa.

To make the photosynthetic parameters obtained at different times comparable to each other, at each measurement period (from 9:30 to 11:30 a.m.), we measured wild-type Yugu 1 at the same time with the mutant lines. Thus, the parameters of Yugu 1 were used as a reference to normalize the photosynthetic parameters of the mutants obtained at different measurement periods. The normalizing formula was as follows:

$A=Y_X/Y_m$

$T=T_X/A$

where Y_X is the photosynthetic data of Yugu 1 at a specific time; Y_m is the mean value of the photosynthetic data of Yugu 1 over all time periods; T_X is the photosynthetic data of the mutant at a specific time period; T is the normalized photosynthetic parameter of the mutant.

Except for Chl content, photosynthetic parameters presented in our text, such as P_n, G_s, and C_i, were all normalized data.

2.4. Data analysis

For statistical analysis, one-way ANOVA followed by an LSD *t*-test was performed to evaluate the difference between Yugu 1 and the mutant lines. Correlation coefficients between all possible pairs of measured parameters were analyzed by Pearson's correlation test. Data analyses were performed with SPSS 17.0. Box and scatter plots were constructed with OriginPro 2019 and R Studio.

3. Results

3.1. Characterization of chlorophyll content of the leaf color mutants

Firstly, as shown in Fig. 1-A, the Chl *a* content of the 28 mutants presented an obvious right-skewed distribution, varying from 1.46 to 2.02 mg dm^{-2} (Appendix A). The Chl *a* content of 18 out of the 28 mutants (64.2%) was significantly lower (P<0.05) than that of the wild-type Yugu 1 (2.02 mg dm^{-2}). Among the 18 mutants with reduced Chl *a* content, 15 mutants (53.6%) showed Chl *a* content slightly reduced to 1.7–1.9 mg dm^{-2}, while three mutants (t53, t68, and t104) showed more markedly reduced Chl *a* contents of 1.45–1.65 mg dm^{-2}. No mutant presented significantly increased Chl *a* content (Fig. 1-A; Appendix A).

Changes in Chl *b* content of the 28 mutants were more striking than those of Chl *a*, and the content varied from 0.41 to 1.38 mg dm^{-2} in what appeared to be a bimodal distribution (Fig. 1-B). The Chl *b* content of wild-type Yugu 1 (0.95 mg dm^{-2}) was very close to the median of the distribution (0.89 mg dm^{-2}). Ten mutants performed significantly higher Chl *b* content than Yugu 1, and 14 mutants performed significantly lower Chl *b* content than Yugu 1. Three mutants, t53, t68, and t104, showed greatly reduced Chl *b* content to half that of Yugu 1, at 0.4575, 0.4723, and 0.4087 mg dm^{-2}, respectively (Fig. 1-B; Appendix A). The total Chl content of t53, t68, and t104 also decreased substantially (Fig. 1-D; Appendix A). Changes in the Chl *a*/*b* ratio were highly correlated with Chl *b* content. As shown in Fig. 1-C, mutants with increased Chl *b* content all presented decreased Chl *a*/*b* ratio, and mutants with decreased Chl *b* content all presented an increased Chl *a*/*b* ratio.

3.2. Characterization of photosynthetic performance of the mutants

As shown in Fig. 2, abundant variations were found among the selected mutants. Compared with the wild type Yugu 1 (in which P_n was 18.24 μmol CO_2 m^{-2} s^{-1}), 23 out of 48 mutants exhibited significantly increased P_n (P<0.05), with the P_n of nine mutants (t53, t34, t57, t54, t17, t58, t103, t39, and t45) exceeding 25 μmol CO_2 m^{-2} s^{-1}, and the P_n of a further nine mutants (t27, t114, t50, t41, t105, t42, t24, t28, and t118) as high as 23–25 μmol CO_2 m^{-2} s^{-1} (Fig. 2-A; Appendix B). In contrast, 12 mutants showed significantly reduced P_n (P<0.05), among which seven mutants (t65, t91, t69, t72, t64, t6, and t66) had P_n lower than 13 μmol CO_2 m^{-2} s^{-1} (Fig. 2-A). The P_n of the remaining 13 mutants showed no significant difference compared with Yugu 1.

As shown in Fig. 2-B, G_s of the selected 48 mutants were in a range of 0.08 to 0.26 mol H_2O m^{-2} s^{-1}. Eleven mutants, namely t6, t14, t20, t89, t10, t95 t86, t11, t8, t50 and t97 performed decreased G_s than that of Yugu 1 ((0.119±0.052) mol H_2O m^{-2} s^{-1}). Moreover, 23 mutants (t81, t58, t30, t68, t66, t69, t17, t26, t93, t105, t41, t28, t27, t114, t34, t24, t118, t23, t54, t42, t103, t45, and t39) behaved with increased G_s when compared of that of Yugu 1. Remarkably, according to the distribution histogram of G_s inserted in Fig. 2-B, G_s of most mutant lines were in a range of 0.08 to 0.26 mol H_2O m^{-2} s^{-1}. Two mutants (t45 and t39) behaved with distinct increases in G_s at 0.227 and 0.2530 mol H_2O m^{-2} s^{-1}. C_i of the selected 48 mutants ranged from 30 to 210 μmol CO_2 mol^{-1}. Moreover, as shown in Fig. 2-C, 12 mutants (t50, t14, t20, t95, t11, t10, t97, t58, t17, t87, t53, and t31) performed decreased C_i, and 21 mutants (t71, t118, t81, t24, t114, t45, t27, t67, t26, t93, t72, t68, t64, t91, t66, t69, t39, t30, t65, t42, and t23) performed increased C_i when compared with Yugu 1.

To further explore the relations among P_n, G_s, and C_i, scatter plots of P_n *vs*. G_s, C_i *vs*. G_s, and P_n *vs*. C_i were made (Fig. 3). Fig. 3-A, D, and G presented scatter plots of P_n *vs*. G_s, C_i *vs*. G_s, and P_n *vs*. C_i, respectively, of the 11 mutant lines with decreased G_s. Fig. 3-B, E, and H presented scatter plots of P_n *vs*. G_s, C_i *vs*. G_s, and P_n *vs*. C_i, respectively, of the 14 mutant lines with unchanged G_s. Fig. 3-C, F, and I presented scatter plots of the 23 mutant lines with increased G_s. Among the 23 mutants with significantly increased G_s (P<0.01), 17 (t17, t23, t24, t26, t27, t28, t34, t39, t41, t42, t45, t54, t58, t103, t105,

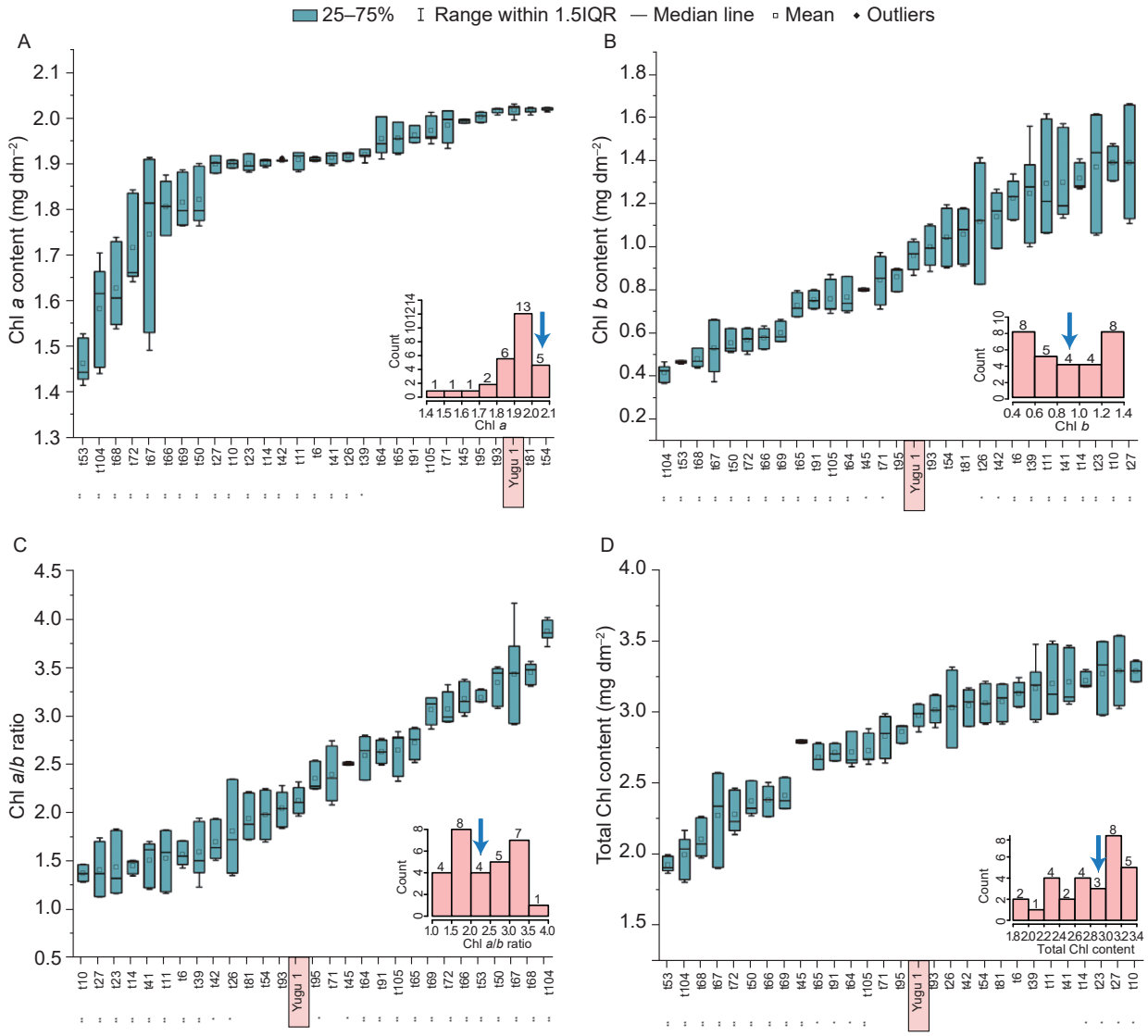

Fig. 1 Chlorophyll (Chl) content of selected 28 leaf-color mutants grown in the field. A, Chl *a*. B, Chl *b*. C, Chl *a*/*b* ratio. D, total Chl content. Insets in the lower right corner of A–D showed frequency distribution histograms of the selected 28 mutants for Chl *a* content, Chl *b* content, Chl *a*/*b*, and total Chl content. *X*-axis was grouped value range of the parameters; *Y*-axis was counts of mutant lines in the value range. Blue arrows indicate the position of wild-type Yugu 1 in the distribution. Values are mean±SE (n=6). Asterisks below the *X*-axis denote significant differences between the indicated mutant and Yugu 1: **, P<0.01; *, P<0.05.

t114, and t118) also showed increased P_n performance (Fig. 3-C, blue "○"). However, three mutants (t30, t81, and t93) exhibited no significant increase in P_n performance (Fig. 3-C, red "Δ"). Three mutants (t66, t68, and t69) showed substantially decreased P_n performance despite their increased G_s (Fig. 3-C, greenblue "+"). Interestingly, C_i was significantly increased in these six mutants (t30, t81, t93, t66, t68, and t69) compared with Yugu 1 (Fig. 3-F).

The G_s of 14 mutants, namely t31, t35, t53, t54, t64, t65, t67, t71, t72, t82, t84, t87, t91, and t104, did not differ significantly from the G_s of Yugu 1 (Fig. 2-B). Thus, the opportunity for the mesophyll cells to capture CO_2 for photosynthesis was equivalent in these mutants and in Yugu 1, and therefore the differences in P_n performance between these mutants and Yugu 1 were largely attributable to non-stomatal factors, such as CO_2 capture and assimilation efficiency. Among the 14 mutants, five mutants (t53, t57, t82, t87, and t104) showed increased P_n performance (Fig. 3-B, blue "○"), five mutants (t64, t65, t67, t72, and t91) showed decreased P_n performance (Fig. 3-B, greenblue "+"), and four mutants (t31, t35, t71, and t84) showed no difference in P_n performance when compared with Yugu 1 (Fig. 3-B, red "Δ"). The five mutants with decreased P_n performance showed significantly increased C_i values (P<0.05), whereas the five mutants with increased P_n performance showed

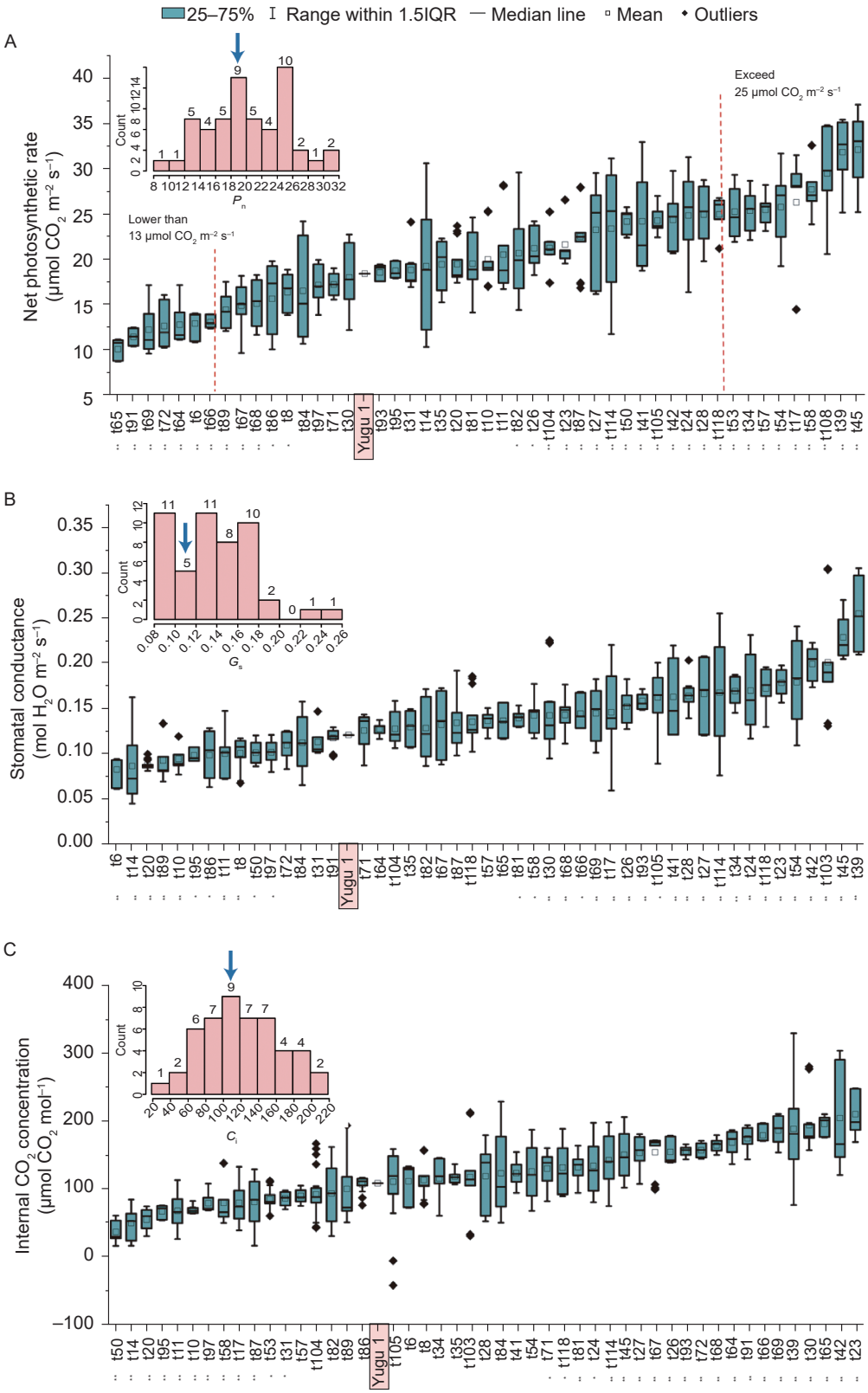

Fig. 2 Net photosynthetic rate (P_n) (A), stomatal conductance (G_s) (B), and internal CO_2 concentration (C_i) of selected 48 mutants grown in the field. Insets in the upper left corner of A–C showed histograms of the frequency distribution of P_n, G_s, and C_i of the selected 48 mutants. *X*-axis was grouped value range of the parameters; *Y*-axis was counts of mutant lines in the value range. Blue arrows indicated the position of wild-type Yugu 1 in the distribution. Error bars represent standard error (n=10). Asterisks below the *X*-axis denote significant differences between the indicated mutant and Yugu 1: **, P<0.01; *, P<0.05.

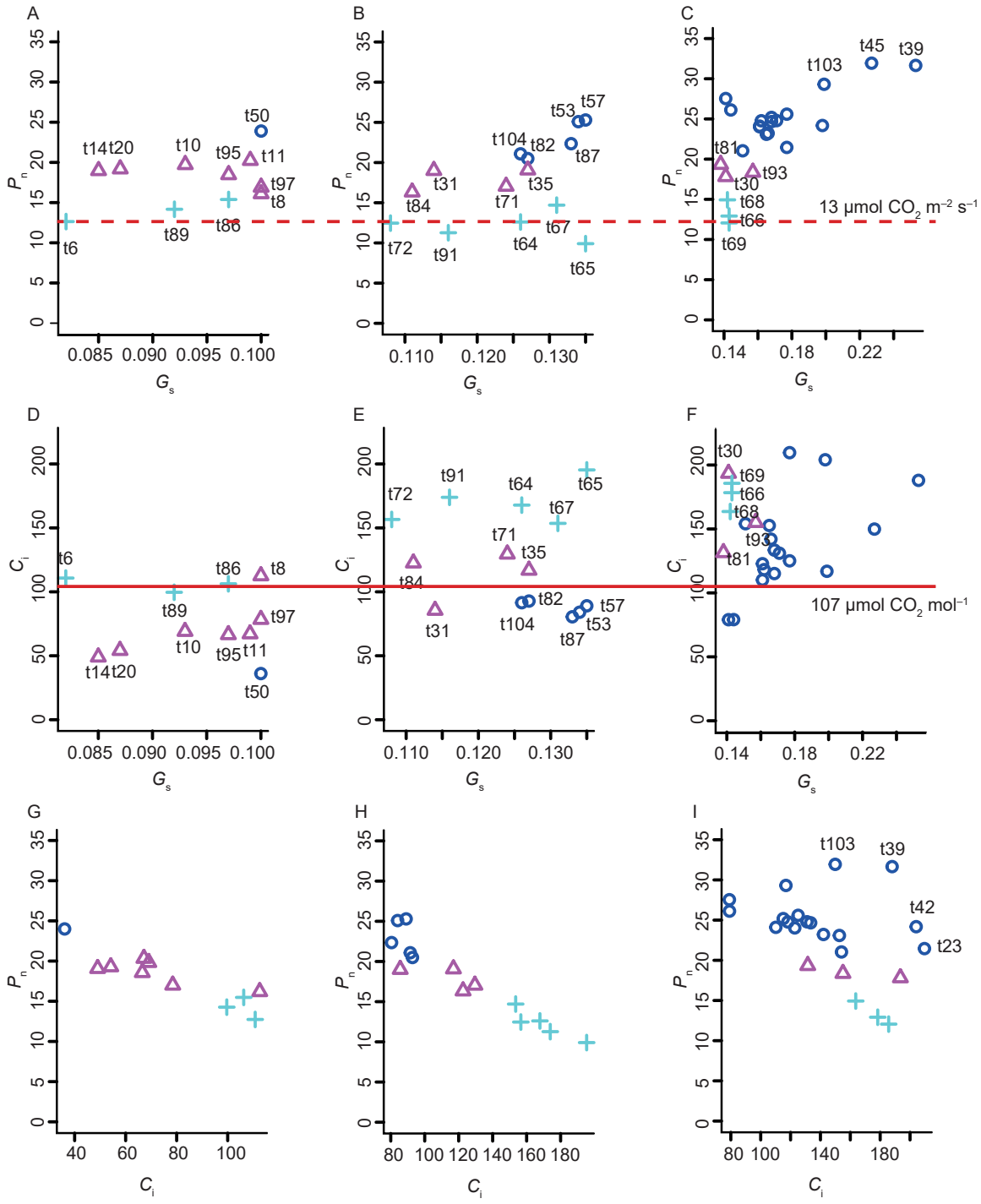

Fig. 3 Scatter plots of net photosynthetic rate (P_n) *vs.* stomatal conductance (G_s), internal CO_2 concentration (C_i) *vs.* G_s, P_n *vs.* C_i of the 48 mutant lines. A–C, scatter plot of P_n *vs.* G_s with mutant lines exhibiting decreased G_s (A), unchanged G_s (B), and increased G_s (C) when comparing with that of Yugu 1. D–F, scatter plot of C_i *vs.* G_s with mutant lines exhibiting decreased G_s (D), unchanged G_s (E), and increased G_s (F) when comparing that of Yugu 1. G–I, scatter plot of P_n *vs.* C_i with mutant lines exhibiting decreased G_s (G), unchanged G_s (H), and increased G_s (I) when comparing that of Yugu 1. Blue "○" represented mutants with increased P_n by comparing with that of Yugu 1; greenblue "+" represented mutants with decreased P_n by comparing with that of Yugu 1; red "△" represented mutants with unchanged P_n by comparing with that of Yugu 1; red dotted line in A–C marked the P_n value of 13 μmol CO_2 m^{-2} s^{-1}; red line in D–F marked the C_i value of Yugu 1 at 107 μmol CO_2 mol^{-1}.

decreased C_i values (Fig. 3-E). These results suggested that C_i and P_n are negatively correlated under consistent G_s conditions (Fig. 3-H).

Furthermore, compared with Yugu 1, there were 11

mutants, namely t6, t8, t10, t11, t14, t20, t50, t86, t89, t95, and t97, with significantly decreased G_s (P<0.05) (Fig. 2-B). The P_n performance of these mutants differed from the wild type (Fig. 3-A). Three mutants (t6, t86, and t89) exhibited decreased P_n in line with their decreased G_s. However, seven mutants (t8, t10, t11, t14, t20, t95, and t97) showed no change in P_n performance despite their decreased G_s. Remarkably, one mutant, t50, showed significantly increased P_n (P<0.01) despite its decreased G_s. Interestingly, the C_i of these seven mutants (t10, t11, t14, t20, t95, t97, and t50) was also significantly decreased compared with Yugu 1 (Figs. 2-C and 3-D). These results indicated that mutant t10, t11, t14, t20, t95, t97, and t50 had increased capacity for capturing CO_2 under decreased G_s.

Moreover, according to Fig. 3-G, H, and I, P_n and C_i were negatively correlated in most cases. However, such a correlation did not exist among the mutant lines with dramatically increased G_s, such as t103, t39, t42, and t23 (Fig. 3-I).

3.3. Correlation analysis between photosynthetic parameters and Chl content

To explore the correlation relationships between the photosynthetic parameters and Chl content, we analyzed the correlations between all possible pairs of measured parameters using Pearson's correlation test. The correlation and scatterplot matrix with the 28 leaf color mutants are shown in Fig. 4. G_s performed the strongest correlation with P_n, with a correlation coefficient of 0.63 (P<0.001). Chl *b* content and Chl *a*/*b* ratio showed a weak correlation with P_n, with coefficients of 0.32 (P<0.1) and –0.31 (P<0.1), respectively. The correlation between C_i and G_s (0.60) was significant (P<0.001). Correlations between Chl *a* and *b* (0.56), Chl *a* and Chl *a*/*b* ratio (0.62), and Chl *b* and Chl *a*/*b* ratio (0.99) were also significant.

To further explore the effect of different levels of G_s and Chl *b* content on P_n, another two scatter plots were constructed in which mutants were grouped into two clusters by different levels of G_s and Chl *b* content, respectively. As shown in Fig. 5-A, blue circles represented mutants with decreased G_s by comparing with Yugu 1. Greenblue plus-signs represented mutants with increased G_s when compared with Yugu 1. Yugu 1 was denoted as a red triangle. It could be concluded that a clear positive linear relationship exists between P_n and G_s within the mutants that behaved with higher G_s than Yugu 1. However, such a linear relationship did not exist among the mutants with decreased G_s. As shown in Fig. 5-A, four mutant lines, t10, t11, t14, and t95, which

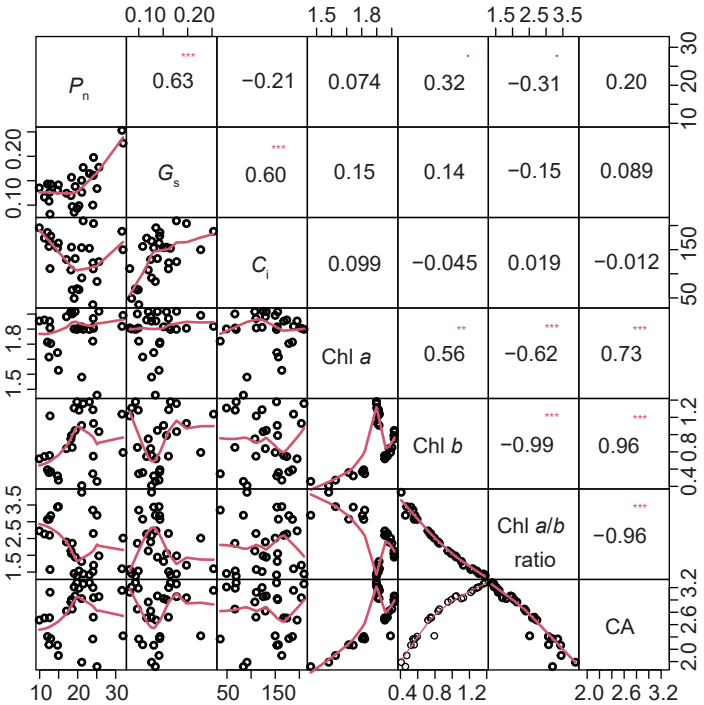

Fig. 4 Correlation and scatterplot matrix. The upper triangular matrix showed a Pearson correlation coefficient between each pair of the measured parameters. The larger font size indicated a stronger correlation. The lower triangular matrix showed the pairwise scatter plots between net photosynthetic rate (P_n), stomatal conductance (G_s), internal CO_2 concentration (C_i), Chl *a*, Chl *b*, Chl *a*/*b* ratio, and total Chl content (CA). Each circle represented a mutant line; red line was the fitting curve of scatter plots; diagonal labels showed the parameters. ***, P-value<0.001; **, P-value<0.01; ·, P-value<0.1.

behaved with significantly decreased G_s compared to Yugu 1, exhibited comparable P_n performance with Yugu 1. Remarkably, one mutant, t50, behaved with significantly decreased G_s but increased Pn compared with Yugu 1.

In fact, among the 23 mutants with significantly increased P_n, 17 (73.9%) showed increased G_s (Fig. 3-A–C); among the 23 mutants with increased G_s, 17 (73.9%) had increased P_n (Fig. 3-C). However, among the 12 mutants with significantly decreased P_n, only four (33.3%) had decreased G_s, five (41.7%) showed no significant change in G_s, and the rest three (25%) had increased G_s (Fig. 3-A–C). In addition, among the seven mutants with markedly decreased P_n (lower than 13 μmol CO_2 m^{-2} s^{-1}), only one (14.3%) exhibited decreased G_s, four (57.1%) had no change in G_s, and two (28.6%) had increased G_s (Fig. 3-A–C). These results suggested that, although increased P_n was mostly attributable to increased G_s, the decreased P_n of most mutants was not attributable to decreased G_s in our study.

Fig. 5-B presented a scatter plot in which mutants were grouped into decreased Chl *b* content cluster and increased Chl *b* content cluster by comparing that of Yugu 1. P_n of most of the mutants with decreased Chl *b* content was lower than that of the mutants with increased Chl *b* content. Interestingly, five mutants, t45, t50, t53, t104, and t105, had decreased Chl *b* content but performed significantly higher P_n when compared with Yugu 1. As t45, t50, and t105 also exhibited variations in G_s (Fig. 2-B), it was hard to determine which factor led to the increased P_n. Thus, two mutants (t53 and t104) were finally identified to perform dramatically decreased Chl *b* content but significantly increased P_n (with no changes on G_s).

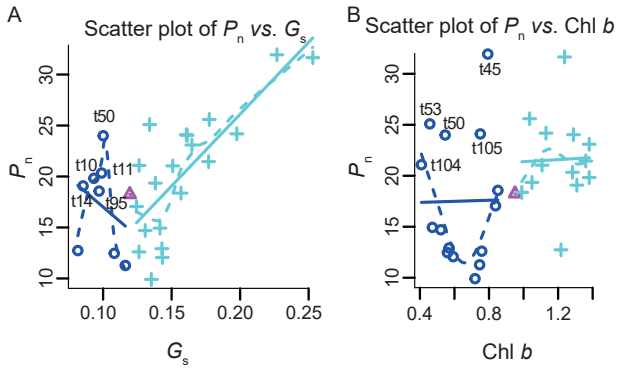

Fig. 5 Grouped scatter and box plots. A, scatter plot of net photosynthetic rate (P_n) *vs*. stomatal conductance (G_s). Blue "○" represented mutants with decreased G_s by comparing with Yugu 1; greenblue "+" represented mutants with increased G_s by comparing with Yugu 1. Yugu 1 was denoted as a red "Δ". B, scatter plot of P_n *vs*. Chl *b*. Blue "○" represented mutants with decreased Chl *b* content by comparing with Yugu 1; greenblue "+" represented mutants with increased Chl *b* content by comparing with Yugu 1. Yugu 1 was denoted as a red "Δ".

4. Discussion

4.1. Chl *b* is an active parameter for photosynthetic modulation

Chl *b* is synthesized from Chl *a* through the activity of chlorophyllide *a* oxygenase (CAO), but increased CAO activity would not increase Chl *b* content at the expense of decreasing Chl *a* content (Biswal *et al.* 2012). In contrast, overexpression of *AtCAO* in tobacco significantly increased not only Chl *b* content but also Chl *a* content and other intermediates involved in Chl biosynthesis (Biswal *et al.* 2012). Other studies in tobacco also showed that overexpression of some of the genes involved in the chlorophyll biosynthesis pathway co-modulated the expression of several other chlorophyll biosynthetic genes (Shalygo *et al.* 2009). In the current study, the Chl content of the 28 *Setaria* mutants was characterized. And a total of 18, 24, and 24 mutants behaved with variations in Chl *a*, Chl *b*, and Chl *a*/*b* ratio, respectively. Chl *a* and *b* contents were positively correlated, suggesting that there was also parallel regulation of Chl *a* and *b* biosynthesis in monocot cereals, such as *Setaria* (Fig. 4). It has been reported that Chl content, especially Chl *b* content, and the Chl *a*/*b* ratio are the key factors that determine the light-harvesting antenna size (Bailey *et al.* 2001). The current study found a small change in Chl *a* content and a more dramatic change in Chl *b* content among the *Setaria* mutants. Moreover, as shown in Fig. 4, weak correlations were found between P_n and Chl *b* content, while such correlations were not found between P_n and Chl *a* content, suggesting that Chl *b* content might be a more responsive indicator than Chl *a* to estimate P_n performance.

4.2. Decreased Chl content mostly leads to decreased P_n, with some exceptions

Generally, increased Chl *b* content represents an enlarged light-harvesting antenna size and thus promotes photosynthesis (Tanaka and Tanaka 2011; Jia *et al.* 2016). Previous studies reported that increased Chl *b* synthesis led to an increased photosynthetic performance in tobacco and *Arabidopsis* (Tanaka *et al.* 2001; Biswal *et al.* 2012). Hu (2009) also reported that there were significant correlations between Chl content and photosynthetic rate in recombinant inbred lines of rice in well-watered conditions (Hu *et al.* 2009). In the current study, we also found a weak correlation between Chl *b* content and P_n (Fig. 4). P_n of most mutants with decreased Chl *b* content (compared with Yugu 1) was lower than that of the mutants with increased Chl *b* content when compared with Yugu 1 (Fig. 5-B). We speculate that the photosystem

of these mutants might resemble those of the *sistl1* and *sistl2* mutants of *Setaria*, which had defects in chloroplast development and chlorophyll biosynthesis (Zhang *et al.* 2018; Tang *et al.* 2019), thus leading to a significant decrease in photosynthesis. However, we also found two mutants (t53 and t104) that had decreased Chl *b* content and unchanged G_s but performed significantly higher P_n when compared with Yugu 1. Previous reports on green algae, tobacco, and soybean showed the prospect of reducing Chl content to improve photosynthesis and yields (Kirst and Melis 2014; Kirst *et al.* 2017). However, similar reports had not yet been seen in other crops. Our study thus provides new evidence that reduced Chl content could also promote photosynthesis in the C_4 crop *Setaria*.

Our study identified various mutants with modulated Chl *b* biosynthesis and P_n. Further investigations on them would ultimately elucidate the relationship between Chl *b* content and photosynthetic performance. Such research would also underpin efforts to modify Chl biosynthesis and the antenna size to improve photosynthesis in *Setaria* and other economically important cereals.

4.3. Promising future for elucidating the high photosynthetic efficiency and water-saving mechanism of C_4 plants

G_s is one of the key factors that greatly affect photosynthesis. Generally, increased G_s strongly correlate with higher P_n (Wong *et al.* 1979; Faralli *et al.* 2019). In this study, a total of 35 mutants were found that had significant variations in P_n, and we also found significant positive correlations between G_s and P_n. Interestingly, correlations between decreased G_s and decreased P_n were found not as evident as the correlation between increased G_s and increased P_n (Fig. 5-A), indicating that decreased G_s would not necessarily lead to decreased P_n in *Setaria*. This might be because *Setaria* is a C_4 plant and thus more tolerant to low CO_2 concentrations and capable of keeping relatively high rates of P_n under restricted G_s.

Drought tolerance is one of the key factors that determine crop productivity (Nowicka *et al.* 2018; Golec *et al.* 2019). Generally, crops tend to reduce G_s to reduce water loss under low soil water conditions, leading to lower P_n and depressed productivity (Gilbert *et al.* 2011). Balancing photosynthetic performance when G_s is restricted is thus a desirable target when breeding drought-tolerant materials (Golec *et al.* 2019). In this study, seven mutants (t50, t10, t11, t14, t20, t95, and t97) had decreased G_s but not decreased photosynthetic performance, indicating that it is possible to develop water-saving *Setaria* cultivars with no evident loss of P_n by balancing G_s and P_n. Our results indicate that *Setaria* is a valuable model crop for elucidating why C_4 species are generally drought-tolerant and water-saving (Diao *et al.* 2014), and the mutants characterized in this study provide fundamental materials for such research.

In addition to the influence of G_s, internal features including the Kranz anatomy and the CO_2 concentrating mechanism of *Setaria* mean it is a model with high photosynthetic efficiency (Li and Brutnell 2011; Diao *et al.* 2014). In this study, 14 mutants did not exhibit significant differences in G_s compared with Yugu 1. Five mutants (t64, t65, t67, t72, and t91) showed decreased P_n while another five mutants (t53, t57, t82, t87, and t104) had increased P_n performance. These mutants, thus, might have variations in the Kranz anatomy and the CO_2 concentrating mechanism that led to different P_n performances. In addition, six mutants (t30, t81, t93, t66, t68, and t69) had increased G_s but not increased P_n, indicating that these mutants might have defects in the Kranz anatomy and CO_2 concentrating mechanism, thus leading to decreased P_n despite more CO_2 flowing into the leaf interior.

In summary, according to the photosynthetic parameters obtained by Li6400 measurements, 17 mutants (t17, t23, t24, t26, t27, t28, t34, t39, t41, t42, t45, t54, t58, t103, t105, t114, and t118; Table 1, category I) behaved with increased P_n and increased G_s, and four mutants (t6, t8, t86, and t89; Table 1, category IX) had decreased P_n and decreased G_s. Eleven mutants had negative variations in photosynthetic characteristics. For example, mutants t30, t81, and t93 showed increased G_s but unchanged P_n (Table 1, category II); t66, t68, and t69 had increased G_s but decreased P_n (Table 1, category III); t64, t65, t67, t72, and t91 had unchanged Gs but decreased P_n (Table 1, category VI). Five mutants had positive variations in photosynthesis, namely t53, t57, t82, t87, and t104, which had unchanged G_s but increased P_n (Table 1, category IV). Remarkably seven mutants behaved with high P_n under restricted G_s conditions. For example, t50 had decreased G_s but increased P_n (Table 1, category VII) and t10, t11, t14, t20, t95, and t97 had decreased G_s but unchanged P_n (Table 1, category VIII). Further investigations on these mutants would be beneficial to elucidate the mechanism of high-efficiency photosynthesis in C_4 plants.

4.4. Perspectives of *Setaria* as a model in photosynthesis research

Factors that strongly limit photosynthesis include the inability to efficiently use midday high light intensities as well as low-intensity light and inefficiency of the catalytic rate

Table 1 Categories of the 48 mutants defined by photosynthetic parameters

Category	Description[1)]	Mutant
I	Increased G_s and P_n	t17, t23, t24, t26, t27, t28, t34, t39, t41, t42, t45, t54, t58, t103, t105, t114, and t118
II	Increased G_s but not changed P_n	t30, t81, and t93
III	Increased G_s but decreased P_n	t66, t68, and t69
IV	Not changed G_s but increased P_n	t53, t57, t82, t87, and t104
V	Not changed G_s and P_n	t31, t35, t71, and t84
VI	Not changed G_s but decreased P_n	t64, t65, t67, t72, and t91
VII	Decreased G_s but increased P_n	t50
VIII	Decreased G_s but not changed P_n	t10, t11, t14, t20, t95, and t97
IX	Decreased G_s and P_n	t6, t8, t86, and t89

[1)] G_s, stomatal conductance; P_n, net photosynthetic rate.

of the carboxylation enzyme Rubisco (Ort *et al.* 2015). To date, numerous strategies have proposed modulating Chl biosynthesis to improve light-use efficiency, some of which have shown positive results in tobacco and *Arabidopsis* (Biswal *et al.* 2012; Kirst *et al.* 2017; Ruban 2017). However, similar results in other crops have not yet been reported. As there appears to be little prospect of improving the kinetic and catalytic features of native Rubiscos, other strategies aimed at improving CO_2 uptake and conversion by increasing stomatal and mesophyll conductance and introducing highly efficient carboxylation systems, like the C_4 photosynthetic pathway, have been proposed for improving photosynthesis (Ort *et al.* 2015). However, because of the complex relationship between Chl biosynthesis, antenna size, and light-use efficiency, as well as the complexity of carbon uptake and conversion mechanisms, many difficulties remain to be overcome in improving photosynthesis, and so further research is required.

Setaria italica, a diploid C_4 panicoid species with small stature, a simple genome, high transformation efficiency, and excellent drought tolerance, has been a useful tool for functional gene mining and research (Diao *et al.* 2014; Huang *et al.* 2014; Doust *et al.* 2019; Nguyen *et al.* 2020; Pegler *et al.* 2020). As it uses the highly efficient C_4 mechanism of photosynthesis, it has been regarded as a useful model for C_4 photosynthesis research (Brutnell *et al.* 2010). Screening for mutants in *Setaria* with a wider range of variation in different photosynthetic characteristics would add benefit to elucidating the mechanisms of C_4 photosynthesis and generating breeding materials with higher photosynthetic rate and water-use efficiency.

5. Conclusion

The current study identified abundant mutants in Setaria with multiple variations in chlorophyll content, stomatal conductance and net photosynthetic rate to provide materials for further investigation, ultimately aiming to establish a drought-tolerant and more efficient photosynthesis mechanism for major crops.

Acknowledgements

This work was supported by the National Natural Science Foundation of China (32241042 and 31771807), the National Key R&D Program of China (2021YFF1000103), the China Agricultural Research System (CARS-06-04), and the Agricultural Science and Technology Innovation Program of the Chinese Academy of Agricultural Sciences. We thank Dr. Huw Tyson, from Liwen Bianji, Edanz Group China (www.liwenbianji.cn/ac), for editing the English text of a draft of this manuscript.

Declaration of competing interest

The authors declare that they have no conflict of interest.

Appendices associated with this paper are available on https://doi.org/10.1016/j.jia.2022.10.014

References

Bailey S, Walters R G, Jansson S, Horton P. 2001. Acclimation of *Arabidopsis thaliana* to the light environment: The existence of separate low light and high light responses. *Planta*, **213**, 794–801.

Biswal A K, Pattanayak G K, Pandey S S, Leelavathi S, Reddy V S, Govindjee, Tripathy B C. 2012. Light intensity-dependent modulation of chlorophyll *b* biosynthesis and photosynthesis by overexpression of chlorophyllide a oxygenase in tobacco. *Plant Physiology*, **159**, 433–449.

Bjorn L O, Papageorgiou G C, Blankenship R E, Govindjee. 2009. A viewpoint: Why chlorophyll *a*? *Photosynth Research*, **99**, 85–98.

Brutnell T P, Wang L, Swartwood K, Goldschmidt A, Jackson D, Zhu X G, Kellogg E, Van Eck J. 2010. Setaria viridis: A model for C_4 photosynthesis. *The Plant Cell*, **22**, 2537–2544.

Chabrand S V , Matthews J S A, Brendel O, Blatt M R, Wang Y, Hills A, Griffiths H, Rogers S, Lawson T. 2016. Modelling water use efficiency in a dynamic environment: An example using *Arabidopsis thaliana*. *Plant Science*, **251**, 65–74.

Chmeliov J, Gelzinis A, Songaila E, Augulis R, Duffy C D, Ruban A V, Valkunas L. 2016. The nature of self-regulation in photosynthetic light-harvesting antenna. *Nature Plants*, **2**, 16045.

Diao X, Schnable J, Bennetzen J L, Li J. 2014. Initiation of Setaria as a model plant. *Frontiers of Agricultural Science and Engineering*, **1**, 16–20.

Doust A N, Brutnell T P, Upadhyaya H D, Eck J V. 2019. Editorial: Setaria as a model genetic system to accelerate yield increases in cereals, forage crops, and bioenergy grasses. *Frontiers in Plant Science*, **10**, 1211.

Faralli M, Lawson T. 2020. Natural genetic variation in photosynthesis: An untapped resource to increase crop yield potential? *Plant Journal*, **101**, 518–528.

Faralli M, Matthews J, Lawson T. 2019. Exploiting natural variation and genetic manipulation of stomatal conductance for crop improvement. *Current Opinion Plant Biology*, **49**, 1–7.

Gilbert M E, Zwieniecki M A, Holbrook N M. 2011. Independent variation in photosynthetic capacity and stomatal conductance leads to differences in intrinsic water use efficiency in 11 soybean genotypes before and during mild drought. *Journal Experimental Botany*, **62**, 2875–2887.

Gitelson A A, Peng Y, Vina A, Arkebauer T, Schepers J S. 2016. Efficiency of chlorophyll in gross primary productivity: A proof of concept and application in crops. *Journal of Plant Physiology*, **201**, 101–110.

Golec A D, Collin A, Sitko K, Janiak A, Kalaji H M, Szarejko I. 2019. Genetic and physiological dissection of photosynthesis in barley exposed to drought stress. *International Journal of Molecular Science*, **20**, 6341.

Horton P, Ruban A. 2005. Molecular design of the photosystem II light-harvesting antenna: photosynthesis and photoprotection. *Journal of Experimental Botany*, **56**, 365–373.

Hu S P, Zhou Y, Zhang L, Zhu X D, Li L, Luo L J, Liu G L, Zhou Q M. 2009. Correlation and quantitative trait loci analyses of total chlorophyll content and photosynthetic rate of rice (*Oryza sativa*) under water stress and well-watered conditions. *Journal of Integrative Plant Biology*, **51**, 879–888.

Huang P, Feldman M, Schroder S, Bahri B A, Diao X, Zhi H. 2014. Population genetics of *Setaria viridis*, a new model system. *Molecular Ecology*, **23**, 4912–4925.

Israel W K, Lazowski W A, Chen Z H, Ghannoum O. 2022. High intrinsic water use efficiency is underpinned by high stomatal aperture and guard cell potassium flux in C_3 and C_4 grasses grown at glacial CO_2 and low light. *Journal of Experimental Botany*, **73**, 1546–1565.

Jeong J, Baek K, Kirst H, Melis A, Jin E. 2017. Loss of CpSRP54 function leads to a truncated light-harvesting antenna size in *Chlamydomonas reinhardtii*. *Biochimica of Biophysica acta Bioenergetics*, **1858**, 45–55.

Jia T, Ito H, Tanaka A. 2016. Simultaneous regulation of antenna size and photosystem I/II stoichiometry in *Arabidopsis thaliana*. *Planta*, **244**, 1041–1053.

Kirst H, Gabilly S T, Niyogi K K, Lemaux P G, Melis A. 2017. Photosynthetic antenna engineering to improve crop yields. *Planta*, **245**, 1009–1020.

Kirst H, Garcia-Cerdan J G, Zurbriggen A, Melis A. 2012. Assembly of the light-harvesting chlorophyll antenna in the green alga *Chlamydomonas reinhardtii* requires expression of the *TLA2-CpFTSY* gene. *Plant Physiology*, **158**, 930–945.

Kirst H, Melis A. 2014. The chloroplast signal recognition particle (CpSRP) pathway as a tool to minimize chlorophyll antenna size and maximize photosynthetic productivity. *Biotechnology Advances*, **32**, 66–72.

Kromdijk J, Głowacka K, Leonelli L, Gabilly S T, Iwai M, Niyogi K K, Long S P. 2016. Improving photosynthesis and crop productivity by accelerating recovery from photoprotection. *Science*, **354**, 851–857.

Kume A, Akitsu T, Nasahara K N. 2018. Why is chlorophyll *b* only used in light-harvesting systems? *Journal of Plant Research*, **131**, 961–972.

Kunugi M, Satoh S, Ihara K, Shibata K, Yamagishi Y, Kogame K, Obokata J, Takabayashi A, Tanaka A. 2016. Evolution of green plants accompanied changes in light-harvesting systems. *Plant & Cell Physiology*, **57**, 1231–1243.

Lawson T, Blatt M R. 2014. Stomatal size, speed, and responsiveness impact on photosynthesis and water use efficiency. *Plant Physiology*, **164**, 1556–1570.

Li P, Brutnell T P. 2011. Setaria viridis and *Setaria italica*, model genetic systems for the Panicoid grasses. *Journal of Experimental Botany*, **62**, 3031–3037.

Li W, Tang S, Zhang S, Shan J, Tang C, Chen Q, Jia G, Han Y, Zhi H, Diao X. 2016. Gene mapping and functional analysis of the novel leaf color gene *SiYGL1* in foxtail millet [*Setaria italica* (L.) P. Beauv]. *Physiologia Plantarum*, **157**, 24–37.

Lichtenthaler H K. 1987. Chlorophylls and carotenoids: pigments of photosynthetic biomembranes. *Methods Enzymol*, **148**, 350–382.

Luo M, Zhang S, Tang C, Jia G, Tang S, Zhi H, Diao X. 2018. Screening of mutants related to the C_4 photosynthetic kranz structure in Foxtail millet. *Frontiers in Plant Science*, **9**, 1650.

Mitra M, Kirst H, Dewez D, Melis A. 2012. Modulation of the light-harvesting chlorophyll antenna size in Chlamydomonas reinhardtii by *TLA1* gene over-expression and RNA interference. *Philosophical Transactions of the Royal Society of London* (Series B: Biological Sciences), **367**, 3430–3443.

Nguyen D Q, Eck J V, Eamens A L, Grof C P L. 2020. Robust and reproducible agrobacterium-mediated transformation system of the C_4 genetic model species setaria viridis. *Frontiers in Plant Science*, **11**, 281.

Nowicka B, Ciura J, Szymańska R, Kruk J. 2018. Improving photosynthesis, plant productivity and abiotic stress tolerance — Current trends and future perspectives. *Journal of Plant Physiology*, **231**, 415–433.

Ort D R, Merchant S S, Alric J, Barkan A, Blankenship R E, Bock R, Hanson M R, Hibberd J M, Long S P, Moore T A, Moroney J, Niyogi K K, Parry M A, Peralta-Yahya P P, Prince R C, Redding K E, Spalding M H, van Wijk K J, Vermaas W F, von Caemmerer S, *et al.* 2015. Redesigning photosynthesis to sustainably meet global food and bioenergy demand. *Proceedings of National Academy of Sciences of the United States of America*, **112**, 8529–8536.

Ort D R, Zhu X, Melis A. 2011. Optimizing antenna size to maximize photosynthetic efficiency. *Plant Physiology*, **155**, 79–85.

Pegler J L, Nguyen D Q, Grof C P L, Eamens A L. 2020. Profiling of the salt stress responsive microrna landscape of C_4 genetic model species *Setaria viridis* (L.) Beauv. *Agronomy*, **10**, 837.

Pinto H, Sharwood R E, Tissue D T, Ghannoum O. 2014. Photosynthesis of C_3, C_3-C_4, and C_4 grasses at glacial CO_2. *Journal of Experimental Botany*, **65**, 3669–3681.

Polle J E, Kanakagiri S D, Melis A. 2003. *Tla1*, a DNA insertional transformant of the green alga *Chlamydomonas reinhardtii* with a truncated light-harvesting chlorophyll antenna size. *Planta*, **217**, 49–59.

Rooijen R V, Aarts M G, Harbinson J. 2015. Natural genetic variation for acclimation of photosynthetic light use efficiency to growth irradiance in Arabidopsis. *Plant Physiology*, **167**, 1412–1429.

Ruban A V. 2017. Crops on the fast track for light. *Nature*, **541**, 36–37.

Shalygo N, Czarnecki O, Peter E, Grimm B. 2009. Expression of chlorophyll synthase is also involved in feedback-control of chlorophyll biosynthesis. *Plant Molecular Biology*, **71**, 425–36.

Siebke K, Ghannoum O, Conroy J P, Caemmerer S V. 2002. Elevated CO_2 increases the leaf temperature of two glasshouse-grown C_4 grasses. *Functional Plant Biology*, **29**, 1377–1385.

Slattery R A, VanLoocke A, Bernacchi C J, Zhu X G, Ort D R. 2017. Photosynthesis, light use efficiency, and yield of reduced chlorophyll soybean mutants in field conditions. *Frontiers in Plant Science*, **8**, 549.

Song Q, Wang Y, Qu M, Ort D R, Zhu X G. 2017. The impact of modifying photosystem antenna size on canopy photosynthetic efficiency — Development of a new canopy photosynthesis model scaling from metabolism to canopy level processes. *Plant*, *Cell & Environment*, **40**, 2946–2957.

Sood P, Singh R K, Prasad M. 2020. An efficient Agrobacterium-mediated genetic transformation method for foxtail millet (*Setaria italica* L.). *Plant Cell Reports*, **39**, 511–525.

Tanaka R, Koshino Y, Sawa S, Ishiguro S, Okada K, Tanaka A. 2001. Overexpression of chlorophyllide a oxygenase (CAO) enlarges the antenna size of photosystem II in *Arabidopsis thaliana*. *The Plant Journal*, **26**, 365–373.

Tanaka R, Tanaka A. 2011. Chlorophyll cycle regulates the construction and destruction of the light-harvesting complexes. *Biochimica et Biophysica Acta*, **1807**, 968–976.

Tang C, Tang S, Zhang S, Luo M, Jia G, Zhi H, Diao X. 2019. SiSTL1, encoding a large subunit of ribonucleotide reductase, is crucial for plant growth, chloroplast biogenesis, and cell cycle progression in *Setaria italica*. *Journal of Experimental Botany*, **70**, 1167–1182.

Tang S, Li L, Wang Y, Chen Q, Zhang W, Jia G, Zhi H, Zhao B, Diao X. 2017. Genotype-specific physiological and transcriptomic responses to drought stress in *Setaria italica* (an emerging model for Panicoideae grasses). *Scientific Reports*, **7**, 10009.

Taylor S H, Aspinwall M J, Blackman C J, Choat B, Tissue D T, Ghannoum O. 2018. CO_2 availability influences hydraulic function of C_3 and C_4 grass leaves. *Journal of Experimental Botany*, **69**, 2731–2741.

Wang P, Grimm B. 2015. Organization of chlorophyll biosynthesis and insertion of chlorophyll into the chlorophyll-binding proteins in chloroplasts. *Photosynthesis Research*, **126**, 189–202.

Wong S C, Cowan I R, Farquhar G D. 1979. Stomatal conductance correlates with photosynthetic capacity. *Nature*, **282**, 424–426.

Zhang S, Tang S, Tang C, Luo M, Jia G, Zhi H, Diao X. 2018. SiSTL2 is required for cell cycle, leaf organ development, chloroplast biogenesis, and has effects on C_4 photosynthesis in *Setaria italica* (L.) P. Beauv. *Frontiers in Plant Science*, **9**, 1103.

Executive Editor-in-Chief ZHANG Xue-yong
Managing Editor WANG Ning